Polarizable interaction potential for molecular dynamics simulations of actinoids(III) in liquid water

Magali Duvail, Fausto Martelli, Pierre Vitorge, and Riccardo Spezia

Citation: The Journal of Chemical Physics **135**, 044503 (2011); doi: 10.1063/1.3613699
View online: http://dx.doi.org/10.1063/1.3613699
View Table of Contents: http://scitation.aip.org/content/aip/journal/jcp/135/4?ver=pdfcov
Published by the AIP Publishing

Polarizable interaction potential for molecular dynamics simulations of actinoids(III) in liquid water

Magali Duvail,[1,a)] Fausto Martelli,[1] Pierre Vitorge,[2] and Riccardo Spezia[3,b)]
[1]*Laboratoire Analyse et Modélisation pour la Biologie et l'Environnement, CNRS UMR 8587, Université d'Evry Val d'Essonne, Boulevard F. Mitterrand, 91025 Evry Cedex, France*
[2]*CEA, DEN, Laboratoire de Spéciation des Radionucléides et des Molécues, F-91991 Gif-sur-Yvette, France*
[3]*CNRS, Laboratoire Analyse et Modélisation pour la Biologie et l'Environnement, CNRS UMR 8587, Université d'Evry Val d'Essonne, Boulevard F. Mitterrand, 91025 Evry Cedex, France*

(Received 1 April 2011; accepted 29 June 2011; published online 25 July 2011)

In this work, we have developed a polarizable classical interaction potential to study actinoids(III) in liquid water. This potential has the same analytical form as was recently used for lanthanoid(III) hydration [M. Duvail, P. Vitorge, and R. Spezia, J. Chem. Phys. **130**, 104501 (2009)]. The hydration structure obtained with this potential is in good agreement with the experimentally measured ion-water distances and coordination numbers for the first half of the actinoid series. In particular, the almost linearly decreasing water-ion distance found experimentally is replicated within the calculations, in agreement with the actinoid contraction behavior. We also studied the hydration of the last part of the series, for which no structural experimental data are available, which allows us to provide some predictive insights on these ions. In particular we found that the ion-water distance decreases almost linearly across the series with a smooth decrease of coordination number from nine to eight at the end. © *2011 American Institute of Physics*. [doi:10.1063/1.3613699]

I. INTRODUCTION

The current renewed interest in nuclear power technology is accompanied by the need for a fundamental understanding of the behavior of the elements involved in the process. In this respect, understanding aqueous chemistry of actinoids (An) and lanthanoids (Ln) has a key role in rationalizing radioactive waste management.[1] Studying structural properties of their hydration is a fundamental first step. Most of the heavier actinoids (from Am) are stable at the 3+ oxidation state in aqueous solutions.[2] Since experimental studies of heavy actinoids are difficult due to their radioactivity and low abundance, lanthanoids are often used as their analogues.[3–6] This corresponds to the usual picture of f-elements as hard cations. Following this picture, their coordination is essentially driven by their charges and ionic radii. By using the hardness limit, we proposed a model which was used to extrapolate a water-cation interaction potential of the whole Ln^{3+} series. We thus obtained hydration behavior in good agreement with experiments.[7]

The hydration structure and dynamics of Ln^{3+} cations is reasonably well established and several experimental and theoretical studies have been devoted to clarify their hydration properties.[8–27] Recently, Persson and co-workers[9] reported a thorough extended x-ray absorption fine structure (EXAFS) study on the whole series in liquid water, providing Ln^{3+}–water distances. There is a trend with respect to the coordination number (CN), which changes from 9 to 8 with a continuous shape in the middle of the series. Our simulations, at the same time, provided a dynamical explanation of the CN changeover across the series[10] in agreement with the experimental trend.

On the other hand, very little structural data have been reported for An^{3+} hydration. Light An^{3+} ions (U^{3+}, Np^{3+}, and Pu^{3+}) are difficult to study experimentally, since they are easily oxidized. However, the hydration structure of U^{3+}, Np^{3+}, and Pu^{3+} was recently reported based on x-ray absorption spectroscopy (XAS).[28] Additionally, experimental hydration energies of U^{3+} and Pu^{3+} have been reported previously by Marcus.[29] The hydration structure of the heavier actinoid cations that are stable in the 3+ oxidation state, from Am^{3+} to the end of the series, is reported experimentally only for Am^{3+}, Cm^{3+}, Bk^{3+}, and Cf^{3+}.[30–35] Cm^{3+} hydration is probably the most investigated among An^{3+} ions, not only by x-ray absorption spectroscopy[32] but also by time resolved laser fluorescence spectroscopy[36] and optical spectroscopy.[37] XAS shows (as expected from ionic radii contraction) a decrease in the An-O distances across the actinoid series, analogous to the Ln^{3+} series. Experimentally CN values reported are not homogeneous, ranging from 8 to 10. It is well known that XAS is very accurate in predicting metal-water distances but CNs are often provided with an uncertainty of ±1. To obtain more reliable CNs, XAS is often coupled with other experimental or theoretical techniques.[38–40] While this was done for many transition metals[39,41–43] and lanthanoids(III),[44,45] there are no coupled systematic studies reported for the whole An^{3+} series in liquid water. Recently, stability, structural parameters, and magnetic behavior were reported for most of the light actinoids(III)–from U to Cm and Cf–by experiments in crystals and theoretical calculations,[46] suggesting that the aqueous chemistry of these An^{3+} ions is very similar to that of the Ln^{3+} ions. Only geometry optimization in implicit solvents were reported on the whole series,[47] but from such

[a)]Present address: PECSA, UPMC, Paris, France.
[b)]Author to whom correspondence should be addressed. Electronic mail: riccardo.spezia@univ-evry.fr. Fax: (+33) 1 69 47 76 55.

studies it is not possible to fully understand hydration structure and dynamics in liquid phase. Results from molecular dynamics simulations based on *ab initio* force fields have shown a CN = 9 for Cm^{3+} at room temperature in water as the prevalent structure,[48–50] in agreement with recent experimental findings.[32,34] Recently, Cf^{3+} was studied by coupling EXAFS with Monte Carlo (MC) calculations in liquid water, suggesting a CN between 8 and 9.[35] Finally, hydration of actinoids with oxidation state 4+ was recently investigated computationally. Notably, a polarizable classical potential parametrized from multi-reference calculations was used for Th^{4+},[51] while the *ab initio* quantum mechanical charge field method was used for U^{4+}.[52]

In this work, we have developed a polarizable potential for An^{3+} hydration providing results in good agreement with available experimental data. We have only considered atoms from U^{3+} to Lr^{3+}, since Th^{3+} and Pa^{3+} are not stable in water and Ac is not strictly speaking an actinoid.[2] In particular, we used the same extrapolation method for the An^{3+} ions that was employed for the Ln^{3+} ions. The validity of this approach was tested by comparison with available experimental data on hydrated An^{3+}. The fact that this extrapolation procedure is successful for An^{3+} ions, which are potentially less hard than their Ln^{3+} analogs, suggests that a purely physical approach is able to reproduce key hydration properties. Moreover, since our model is based on ionic radii and polarizability behavior across the series, we are able to study not only the lighter actinoid ions for which experiments are available but also the heavier members of the series for which no experimental structural results are available. As suggested from the few published experiments, the ion-water distance decreases across the series and the coordination number changes from nine (for light atoms) to eight (for heavy atoms) in a smooth way. Finally, we have calculated hydration enthalpies and compared our results with experimental values[29] and values obtained from a thermodynamic model.[53]

The outline of the reminder of the text is as follows. We first describe the potential development (Sec. II A) and the computational details employed (Sec. II B). Next, we show results for the light atoms and compare them with experimental data (Sec. III A) and then what our model predicts for the heavier atoms at the end of the series for which no structural experimental data are available (Sec. III B). In Sec. III C we report hydration enthalpies as obtained for the whole series and compare with available published data. Section IV summarizes and concludes our findings.

II. DEVELOPING WATER-ACTINOIDS(III) INTERACTION POTENTIAL

A. Theory

The total potential energy of our system is modeled as a sum of different terms,

$$V_{tot} = V_{elec} + V_{O-O}^{LJ} + V_{An-O}, \tag{1}$$

where V_{elec} is the electrostatic energy term composed of a Coulomb and a polarization term following Thole's induced dipole model.[54] V_{O-O}^{LJ} is the 12-6 Lennard-Jones potential describing the O-O interaction. Because of the explicit polarization introduced in the model, the original TIP3P water[55] was modified into the TIP3P/P water model,[56] i.e., the charges on O and H were rescaled to reproduce correctly the dipole moment of liquid water. Atomic polarizability directly enters in the polarization part of the electrostatic energy term and we use values obtained from *ab initio* calculations as detailed in Subsection II B.

V_{An-O} account for the *non-electrostatic* An-O interaction potential. We have chosen a potential composed by a long range attractive part with a $1/r^6$ behavior and a short range repulsive part modeled via an exponential function, dealing with the well-known potential,

$$V_{An-O} = A_{An-O} \exp(-B_{An-O} r_{An-O}) - \frac{C_{An-O}}{r_{An-O}^6}. \tag{2}$$

Note that our previous study of La^{3+} hydration properties pointed out that this analytical expression of the non-electrostatic interaction reproduced well the experimental data.[7,57] This could be not only due to the higher flexibility of the exponential expression of the repulsive term but also to the more physically realistic basis of the exponential form in treating short-range interactions.[58,59] In fact, most of the newly developed interaction potentials, with or without polarizability, often uses an exponential term to describe the short-range repulsion.[60–63] Three parameters determine the energy values of the Buckingham potential: A_{ij}, B_{ij}, and C_{ij}. The first parameter, A_{ij}, represents the height of the repulsion. This value is a fictitious value that for La^{3+} is $1.004 \times 10^{+6}$ kJ/mol^{-1}, corresponding to energies larger than those explored in liquid phase. Thus, as often done in classical parametrizations, it is kept fixed throughout the series. The other two terms can be connected to the variation of ionic radii across the series. We proceed as in our previous work[7] where we used an empirical expression to connect B_{ij} with differences in ionic radius with respect to a reference B value (B_{ref}),

$$B_{ij} = B_{ref} - k\Delta r, \tag{3}$$

where $B_{ref} = B_{LaO} = 3.48$ Å^{-1} and $k = 1$ Å^{-2}. Also C_{ij} terms were modified following the behavior of ionic radii across the series. They were obtained graphically assuming that the heights of the repulsion walls are the same for every system, and then the new interaction potential curves are shifted towards smaller value considering difference in ionic radius with respect to the La^{3+} that is taken as reference. These assumptions were validated for lanthanoids(III) (Ref. 7) and the good agreement found between our simulations and experiments is a further validation of this extrapolation method. Note that this attempt to construct a potential which systematically depends on lanthanoid radii was also done by Madden and co-workers in the case of molten salts.[62,64,65] Moreover, a justification of the dependence of the potential on an atomic parameter, identified here with the

ionic radius difference with respect to a reference value, is given in the Appendix.

In the case of lanthanoids(III), Shannon ionic radii were available for the whole series.[66] Unfortunately, for actinoids(III) less data are present. Shannon reported data, obtained from solid state experiments, across the actinoid(III) series only for CN = 6, and a value for Am^{3+} with CN = 8. As reported for Ln^{3+}, ionic radius increases as CN increases for a given ion. Across the lanthanoid(III) series, ionic radii corresponding to CN = 8 (r_8) and CN = 9 (r_9) decrease from light to heavy ions almost linearly and the two curves are roughly parallel to each other and to the one corresponding to CN = 6. We assumed the same behavior to estimate the ionic radii of the whole An^{3+} series. An intermediate set of parameters ($r_{8.5}$) can also be obtained by averaging CN = 9 and CN = 8 ionic radii. This corresponds to a situation where there is a coexistence of two stoichiometries, such that the effective ionic radius is in between CN = 9 and CN = 8, as suggested for Gd^{3+}.[45]

B. Computational details

Simulations of hydrated An^{3+} ions have been carried out in the microcanonical *NVE* ensemble with our own developed classical molecular dynamics (CLMD) code MDVRY,[67] using the extendend Lagrangian method to propagate induced dipoles in time.[68] The induced dipoles are obtained at the beginning of the dynamics through the resolution of the self-consistent equation,

$$\mathbf{p_i} = \bar{\bar{\alpha}}_\mathbf{i} \cdot \left(\mathbf{E_i} + \sum_{\mathbf{i \neq j}} \bar{\bar{\mathbf{T}}}_\mathbf{ij} \cdot \mathbf{p_j} \right), \tag{4}$$

where $\mathbf{p_i}$ is the induced dipole associated with an isotropic atomic polarizability tensor $\bar{\bar{\alpha}}_i$, following Thole's induced dipole model[54] and

$$\bar{\bar{T}}_{ij} = \frac{1}{r_{ij}^3} \left(\bar{\bar{1}} - 3 \frac{\bar{\bar{A}}_{ij}}{r_{ij}^2} \right), \tag{5}$$

$$\bar{\bar{A}}_{ij} = \begin{pmatrix} (x_i - x_j)^2 & (x_i - x_j)(y_i - y_j) & (x_i - x_j)(z_i - z_j) \\ (x_i - x_j)(y_i - y_j) & (y_i - y_j)^2 & (y_i - y_j)(z_i - z_j) \\ (x_i - x_j)(z_i - z_j) & (y_i - y_j)(z_i - z_j) & (z_i - z_j)^2 \end{pmatrix}. \tag{6}$$

The resolution of this self-consistent problem rapidly becomes extremely time consuming as the system grows. Thus, to reduce computing time, we have used a Car-Parrinello type dynamics of additional degrees of freedom associated with induced dipoles.[68] The Hamiltonian of the system becomes

$$\mathcal{H} = V + \frac{1}{2} \sum_i m_i \mathbf{v_i^2} + \frac{\mathbf{1}}{\mathbf{2}} \sum_\mathbf{i} \boldsymbol{m}_{\mathbf{p_i}} \mathbf{v}_{\mathbf{p_i}}^\mathbf{2}, \tag{7}$$

where V is the total potential, $\mathbf{v_i}$ is the velocity of the atom i, $\mathbf{v_{p_i}}$ is the velocity of the induced dipole $\mathbf{p_i}$ treated as an additional degree of freedom in the dynamics, and $m_{\mathbf{p_i}}$ is the dipole fictitious mass connected to characteristic frequency of the induced dipole $\omega_{\mathbf{p_i}} = 2\pi/\tau = 1/\sqrt{m_{\mathbf{p_i}} \alpha_i}$ with $\tau = 0.005$ ps for each atomic site. Note that the dynamics of the induced dipole degrees of freedom is fictitious, such that it only serves the purpose of keeping the induced dipoles close to their values at minimum energy (that would be obtained through the exact resolution of self-consistent equation at each step). This was verified on some snapshots of the present simulations (induced dipoles obtained with self-consistent field (SCF) are within the oscillations observed using the dipole dyamics), while a more detailed report of the performances of the extended Lagrangian implementation is reported elsewhere.[67]

Each of the CLMD simulations consist of one An^{3+} ion and 216 rigid water molecules in a cubic box at room temperature. As previously reported, CLMD simulations with a 1000 water molecules box provide the same cation structural and dynamical hydration properties as the simulations with 216 water molecules.[57] Therefore, simulations with 216 water molecules were used in the present study to assess An^{3+} hydration properties.

Periodic boundary conditions were applied to the simulation box. Long-range interactions were calculated by using the smooth particle mesh Ewald method.[69] Simulations were performed using a velocity-verlet-based multiple time scale for the simulations with the TIP3P/P water model. Equations of motion were numerically integrated using a 1 fs time step. The system was equilibrated at 298 K for 2 ps. Production runs were subsequently collected for 3 ns. All simulation details are the same as reported previously.[7,10,57,70,71] Initial configurations were built from an equilibrated box with 216 water molecules in which the ion was placed at the center of the box.

Ab initio calculations were performed using the GAUSSIAN-98 package[72] at the second-order Møller-Plesset perturbation (MP2) level of theory. The actinoids were described by the ECP60MWB-SEGg2h basis set and the corresponding electron core potentials.[73,74] ECP60MWB-SEGg2h is obtained from ECP60MWB-SEG where two of the original diffuse g functions were kept and one h function was added. Using the MP2/ECP60MWB-SEGg2h method to obtain actinoid polarizabilities, we were able to reproduce values for Th^{4+}, Pa^{4+}, and U^{4+} previously calculated employing relativistic methods[75] within 2% or less. We are thus confident in the values obtained for An^{3+} for which no data on ionic polarizabilities are reported in the literature.

TABLE I. Estimated ionic radii, IR (in Å), with corresponding B (in $Å^{-1}$) and C (in kJ mol^{-1} $Å^6$) parameters. Also polarizabilities, α, are reported (in $Å^3$).

Ion	IR	B	$C/10^{+4}$	α
$U^{3+}_{(9)}$	1.213	3.483	3.7464	1.846
$Np^{3+}_{(9)}$	1.196	3.500	3.6384	1.633
$Pu^{3+}_{(9)}$	1.179	3.517	3.5342	1.486
$Am^{3+}_{(9)}$	1.162	3.534	3.4334	1.363
$Cm^{3+}_{(9)}$	1.145	3.551	3.3359	1.238
$Bk^{3+}_{(9)}$	1.128	3.568	3.2418	1.197
$Bk^{3+}_{(8.5)}$	1.101	3.596	3.0953	1.197
$Bk^{3+}_{(8)}$	1.073	3.623	2.9573	1.197
$Cf^{3+}_{(9)}$	1.110	3.586	3.1455	1.166
$Cf^{3+}_{(8.5)}$	1.083	3.613	3.0086	1.166
$Cf^{3+}_{(8)}$	1.056	3.640	2.8752	1.166
$Es^{3+}_{(9)}$	1.093	3.603	3.0572	1.154
$Es^{3+}_{(8.5)}$	1.066	3.630	2.7934	1.154
$Es^{3+}_{(8)}$	1.038	3.658	2.7916	1.154
$Fm^{3+}_{(9)}$	1.076	3.620	2.9719	1.174
$Fm^{3+}_{(8.5)}$	1.049	3.647	2.839	1.174
$Fm^{3+}_{(8)}$	1.021	3.675	2.7150	1.174
$Md^{3+}_{(9)}$	1.059	3.637	2.8895	1.063
$Md^{3+}_{(8.5)}$	1.032	3.664	2.7616	1.063
$Md^{3+}_{(8)}$	1.004	3.692	2.6409	1.063
$No^{3+}_{(9)}$	1.042	3.654	2.7911	0.999
$No^{3+}_{(8.5)}$	1.015	3.682	2.6815	0.999
$No^{3+}_{(8)}$	0.987	3.709	2.5690	0.999
$Lr^{3+}_{(9)}$	1.025	3.671	2.7325	0.909
$Lr^{3+}_{(8.5)}$	0.998	3.699	2.6126	0.909
$Lr^{3+}_{(8)}$	0.970	3.726	2.4995	0.909

All the parameters obtained and subsequently used in CLMD simulations are reported in Table I.

III. HYDRATION PROPERTIES IN BULK WATER

An^{3+} hydration has been studied experimentally from U^{3+} to Cf^{3+} , while from Es^{3+} to Lr^{3+} there are no structural data reported experimentally. Thus we first show our CLMD results for the first part (here defined as light actinoids(III)) and then, based on the confidence we get from the agreement between simulations and experimental results, we show results for the second part (heavy actinoids(III)). In Fig. 1 we report a snapshot from a simulation showing a typical simulation box used, where water molecules in first shell are highlighted. Note that the ion-water interaction potential formula does not depend on the situation of the water molecule (i.e., does not change in its expression if the water molecule is in first or second hydration shell or in the bulk).

A. U^{3+}–Cf^{3+} hydration

We first report the hydration structure for light actinoids(III) obtained from CLMD simulations and compare

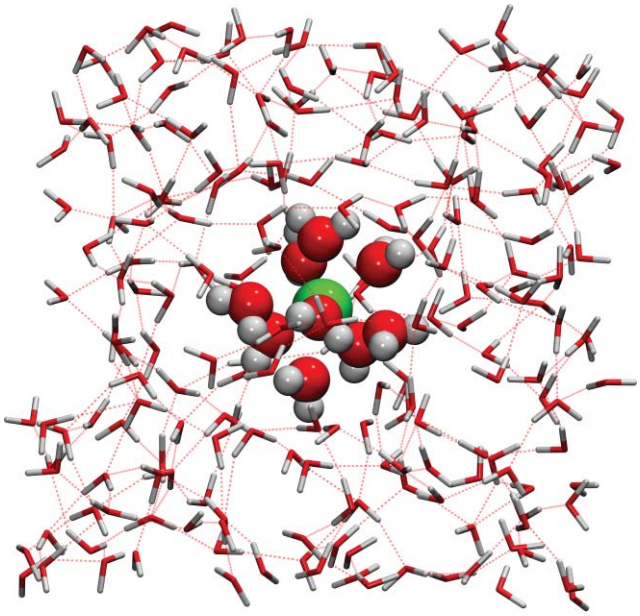

FIG. 1. A snapshot showing an actinoids(III) cation (in green) surrounded by water molecules. The first hydration shell is shown in spheres (red for oxygen, white for hydrogen), while bulk water is shown as sticks. The H-bond network is also shown with dashed lines.

our results with experimental (and some simulation) results from the literature. The structure around An^{3+} cations is first analyzed in terms of An-water radial distribution functions (RDF). In Fig. 2 we show, as an example, RDF for U^{3+}, Cm^{3+}, and Cf^{3+}. We have chosen three ions in the series that were studied experimentally by XAS techniques that could give us structural information. Cm^{3+} and Cf^{3+} were also studied by different theoretical approaches.[35,48–50] From the RDFs we can extract the first and second hydration shell ion-water distances, $r^{(1)}_{An-O}$ and $r^{(2)}_{An-O}$. Additionally, by integration of the RDFs up to the first (r_{min1}) and second (r_{min2}) minima, the first and second shell coordination numbers, $CN^{(1)}$ and $CN^{(2)}$, respectively, can be calculated as follows:

$$CN^{(1)} = 4\pi\rho \int_0^{r=r_{min1}} g(r) r^2 dr, \tag{8}$$

$$CN^{(2)} = 4\pi\rho \int_{r=r_{min1}}^{r=r_{min2}} g(r) r^2 dr. \tag{9}$$

In Fig. 2 we also show the integrated RDF providing CN as a function of distance. $CN^{(1)}$ corresponds to the plateau after the first RDF peak. The first shell is very well structured, as expected, similar to Ln^{3+} in water and also to other very heavy metal cations like U^{4+} and Th^{4+}.[51,52] The high structuration of the first shell induces a structuration of the second shell as well (of course to a lesser extent).

In Table II we report all structural results obtained with our models and compare them with available experimental and theoretical data present in the literature. Our calculated An-O distances are in very good agreement with the experimental values, thus validating our force field on the first part of the series. In particular, we reproduce well the experimental water-cation distances of U^{3+} (2.51 vs. 2.52(1) Å (Ref. 28)), Np^{3+} (2.50 vs. 2.51(1) Å (Ref. 28)), Pu^{3+} (2.49 vs. 2.49(1) Å

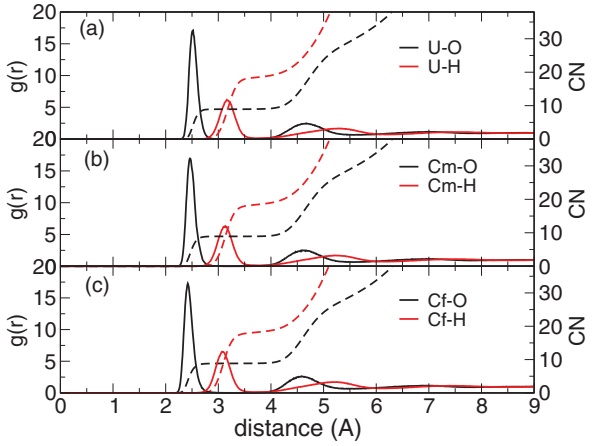

FIG. 2. An-O (in black) and An-H (in red) RDFs with corresponding CNs (dashed lines) for U^{3+} (panel a), Cm^{3+} (panel b), and Cf^{3+} (panel c).

(Ref. 28)), Am^{3+} (2.48 vs 2.480(6) Å (Ref. 30)), Bk^{3+} (2.43 vs 2.43(2) Å (Ref. 31)), and Cf^{3+} (2.42 vs 2.42(1) Å (Refs. 33 and 35)) as obtained from different experiments. For Pu^{3+} the distance reported by Allen *et al.*,[30] 2.510(6) Å, is slightly longer than what we obtained, while we are in very good agreement with the value reported by Brendebach *et al.*[28] The Cm-O distance is within the data spread obtained by different experiments[30,32,34] and in good agreement with previous simulations.[48,49] Note also that the second shell peak is very similar to what has been obtained by MD simulations using interaction potentials derived from complete active space SCF/complete active space with second-order perturbation theory (CASPT2),[49] density functional theory,[48] and Hartee-Fock[50] calculations.

We have found (and shown) that the r_9 parameters describe well systems from U^{3+} to Cm^{3+}. In the case of Bk^{3+} both r_9 and r_8 parameters show some differences with respect to experimental values. We have thus introduced $r_{8.5}$ parameters, which correspond to an effective ionic radius in between CN = 9 and CN = 8, and better reproduce the experimental values.

We should pause here and provide some comments on the use of Shannon ionic radii to derive the non-electrostatic force field parameters. Shannon radii are obtained in the solid state and they correspond to rigid structures. In liquid water the situation is very different. At this end some authors have suggested "effective" ionic radii in water for lanthanoids(III) that do not show a monotonic decreasing across the series as obtained in the solid state.[12,76] The radii of Ln^{3+} in liquid water were recently measured by D'Angelo *et al.*[77] from an accurate EXAFS analysis, where the expected nearly linear behavior with respect to atomic number was found.

In the case of actinoids(III) the same procedure to obtain effective ionic radii across the series is not possible, since accurate EXAFS signals are not available for the whole series. Thus, we used Shannon ionic radii, conscious of the possible limitations of using solid state data for solution phase. For An(III) Shannon reported some values for CN = 6 and a value for CN = 8 (for Am^{3+}). Based on these values and assuming that for each given An^{3+} ionic radius increases as a function of CN (as noticed for Ln^{3+}),[7] we have inferred ionic radii corresponding to CN = 8 and CN = 9 (r_8 and r_9). The "intermediate" $r_{8.5}$ values are obtained by averaging r_8 and r_9, and this corresponds to a situation that is "intermediate" between CN = 8 and CN = 9. Note that here and in previous studies[7,45] on Ln^{3+}, we found that when r_8 (or r_9) are used to derive the potential, the following simulations do not necessarily give as results the corresponding CN (e.g., Lu^{3+} with r_9 parameters provided CN = 8.2). Here we considered different sets of derived ionic radii and then compared the results to experiments in order to find the best parameters for each An^{3+} for which structural data are available, thus adopting an empirical approach. Then, as described in Subsection III B, the parameters were extended to heavy actinoids(III).

In Table II we also report the first ($CN^{(1)}$) and second ($CN^{(2)}$) hydration shell coordination numbers, obtained by integrating An-O RDFs. In the case of actinoids(III) in the U-Cf range, for which structural experimental data are reported, CN = 9, and is almost constant across the series. For Cf^{3+}, the heaviest ion for which XAS experiments are

TABLE II. Hydration properties of light An^{3+} obtained from CLMD. For Bk^{3+} and Cf^{3+} results with different sets of parameters are also shown.

Ion	Method	$r^{(1)}_{An-O}$	$CN^{(1)}$	$r^{(2)}_{An-O}$	$CN^{(2)}$
U^{3+}	CLMD (r_9)	2.51	9.01	4.67	21.1
	EXAFS[a]	2.52	9.1		
Np^{3+}	CLMD (r_9)	2.50	9.00	4.66	20.9
	EXAFS[a]	2.50-2.52	9-10		
Pu^{3+}	CLMD (r_9)	2.49	9.00	4.65	21.6
	EXAFS[a]	2.49	9.9-10		
	EXAFS[b]	2.51	9		
Am^{3+}	CLMD (r_9)	2.48	9.00	4.64	21.2
	EXAFS[b]	2.48	10		
Cm^{3+}	CLMD (r_9)	2.46	9.00	4.62	20.8
	EXAFS[b]	2.45	10		
	EXAFS[c]	2.47	9		
	EXAFS[d]	2.48	8.5		
	MD-NEMO[e]	2.55	8.9	4.9	
	MD[f]	2.48	9	4.65	21
	AIMD[g]	2.50	9	4.71	15.8
	CLMD-3B[g]	2.53	9	4.70	17.4
	CLMD-LJ[g]	2.52	9	4.70	16.4
Bk^{3+}	CLMD (r_9)	2.46	8.99	4.63	20.6
	CLMD (r_8)	2.41	8.91	4.58	20.0
	CLMD ($r_{8.5}$)	2.43	8.98	4.60	20.9
	EXAFS[h]	2.43	9		
Cf^{3+}	CLMD (r_9)	2.44	8.98	4.62	21.0
	CLMD (r_8)	2.39	8.76	4.56	19.9
	CLMD ($r_{8.5}$)	2.42	8.92	4.59	20.0
	EXAFS[i]	2.42	8.5		
	MC[j]	2.43/2.53	7.5/8.8	4.65/4.69	16-17/18-19

[a]XAS data of Brendebach *et al.* (Ref. 28).
[b]EXAFS of Allen *et al.* (Ref. 30).
[c]EXAFS of Skanthakumar *et al.* (Ref. 32).
[d]EXAFS of Lidqvist-Reis *et al.* (Ref. 34).
[e]Simulations of Hagberg *et al.* (Ref. 49).
[f]Simulations of Yang and Bursten (Ref. 48).
[g]Simulations of Atta-Fynn *et al.* (Ref. 50), AIMD is *ab initio* molecular dynamics, CLMD-3B and CLMD-LJ are classical molecular dynamics with a 3-body and Lennard-Jones potential respectively.
[h]EXAFS of Antonio *et al.* (Ref. 31).
[i]EXAFS of Revel *et al.* (Ref. 33).
[j]Monte Carlo simulations of Galbis *et al.* (Ref. 35).

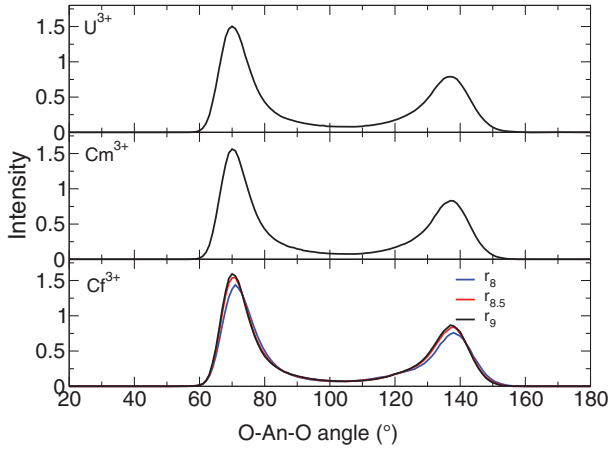

FIG. 3. ADF of O-An-O in the first hydration shell for U^{3+}, Cm^{3+}, and Cf^{3+}. For Cf^{3+} r_9, $r_{8.5}$, and r_8 parameters results are shown.

reported, we have obtained a coordination number of 8.9, corresponding to a large predominance of ninefold coordination structure. As already noted, XAS provides the distances of scattering atoms around the photo-absorber atom (here oxygen atoms and An^{3+}, respectively) with a very good accuracy, but the number of scattering atoms is not given with the same accuracy. Experiments reported on An^{3+} have been interpreted with CNs in the 8–10 range. Note that different experiments on the same An^{3+} ion provide different CN values in this range: Cm^{3+} experiments report CN between 8 and 10 range,[30,32] for U^{3+}, Pu^{3+}, and Am^{3+} they report values between 9 and 10 (Refs. 28 and 30) and finally for Cf^{3+} values between 8 and 9.[35]

In Fig. 3 we show the angular distribution functions (ADFs) obtained for U^{3+}, Cm^{3+}, and Cf^{3+}. The ADF reports the distribution of angles formed between oxygen atoms of water molecules in first An^{3+} hydration shell and the central cation, providing a useful information on the three-dimensional arrangement of water molecules around the central cation. For light actinoids(III), the RDFs consist of two main peaks that corresponds to a trigonal tricapped prism (TTP) structure, similarly to what was obtained for Ln^{3+}. For Cm^{3+} we show the ADFs obtained with different simulations (r_9, $r_{8.5}$, and r_8). They all have two main peaks and thus represent similar structures, confirming that the Cm^{3+} hydration is a 9-fold TTP-like structure. This also shows the robustness of the parameters employed, since the results are only little sensitive to relatively small changes in parameters.

Before moving to heavier actinoids(III), for which no experimental structural data are present, we discuss the effect of ionic polarizability on results. While for Ln^{3+} there are experimental values that we used[78] and which are similar to theoretical values,[79] for An^{3+} no experiments or calculations are currently available. Thus we used *ab initio* calculations to estimate the polarizabilities for An^{3+} . In our previous study on Ln^{3+} we have shown that Ln polarizability has a minor role.[7] Here we obtain similar behavior for An^{3+}. In particular, as shown in Table III, we performed a sensitivity test by multiplying the original Cm^{3+} polarizability (1.238 $Å^3$) by one, two, and three, i.e., we have modified Cm^{3+} polarizability in the 1.238–3.714 $Å^3$ range, showing that Cm-O distances are relatively unaffected (0.03 Å) and the CN is unchanged. This robustness of results on modification of ionic polarizability in a reasonable range further strengthens our confidence in the interaction model.

TABLE III. Hydration properties of Cm^{3+} as a function of ionic polarizability.

α ($Å^3$)	$r^{(1)}_{Cm-O}$ (Å)	$CN^{(1)}$	$r^{(2)}_{Cm-O}$ (Å)	$CN^{(2)}$
1.238	2.46	9.00	4.62	20.8
2.476	2.48	9.00	4.65	20.8
3.714	2.49	9.00	4.65	20.8

B. Es^{3+}–Lr^{3+} hydration

We finally move to hydration of heavy actinoids(III), for which no structural data are available. We report in Table IV the distances and coordination numbers obtained by the different sets of parameters corresponding to the extension of effective ionic radii to the heavy actinoids. The An-O distances show only minor fluctuations (0.025–0.03 Å), comparable to experimental uncertainty, for each species when parameters are changed from r_9 to r_8. Also for CN the values obtained from different parameters have a spread decreasing from Es^{3+} to Lr^{3+}. The RDFs for Lr^{3+} are shown in Fig. 4 and demonstrate that Lr^{3+} has a coordination number of 8. Combining CN = 8 with the shape of ADF, also shown in Fig. 4, we conclude that for Lr^{3+} the hydration structure is similar to that of Lu^{3+}.[7] As previously remarked, there are no experimental data on hydration structure for atoms at the end of the series, but only *ab initio* structures of $[An^{III}(OH_2)_h]^{3+}$ clusters optimized for different values of *h* (7-9) within an implicit solvent have been reported.[47] We found that our distances are slightly shorter than what was obtained by these *ab initio* calculations (by about 0.1 Å depending on the actinoid and *h*). However, *ab initio* calculations overestimate distances by about the same amount with respect to experiments for lighter

TABLE IV. Hydration properties of heavy An^{3+} obtained from CLMD with different parameter sets (r_9, r_8, and $r_{8.5}$).

Ion	Method	$r^{(1)}_{An-O}$	$CN^{(1)}$	$r^{(2)}_{An-O}$	$CN^{(2)}$
Es^{3+}	CLMD (r_9)	2.43	8.94	4.59	20.3
	CLMD ($r_{8.5}$)	2.40	8.84	4.57	19.7
	CLMD (r_8)	2.37	8.52	4.55	19.3
Fm^{3+}	CLMD (r_9)	2.41	8.86	4.58	20.6
	CLMD ($r_{8.5}$)	2.38	8.63	4.56	19.9
	CLMD (r_8)	2.35	8.29	4.53	19.1
Md^{3+}	CLMD (r_9)	2.39	8.67	4.56	19.7
	CLMD ($r_{8.5}$)	2.36	8.36	4.53	19.9
	CLMD (r_8)	2.34	8.12	4.50	19.1
No^{3+}	CLMD (r_9)	2.36	8.34	4.53	19.3
	CLMD ($r_{8.5}$)	2.34	8.18	4.51	19.0
	CLMD (r_8)	2.32	8.03	4.49	19.3
Lr^{3+}	CLMD (r_9)	2.34	8.14	4.51	18.7
	CLMD ($r_{8.5}$)	2.33	8.07	4.50	19.1
	CLMD (r_8)	2.31	8.00	4.48	18.8

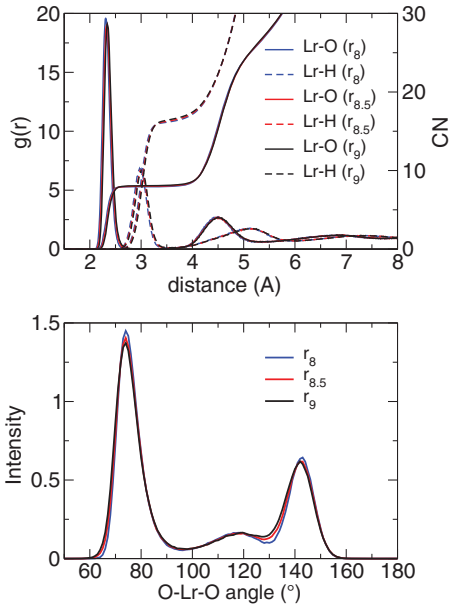

FIG. 4. Lr-O and Lr-H RDFs (upper panel) and O-Lr-O ADF (lower panel) for the different set of parameters.

actinoids(III). Further, when an explicit water molecule is added in the second hydration shell, a shortening in the An-O distances was found. Unfortunately, as often happens with these approaches,[80] these *ab initio* calculations cannot provide decisive conclusions on coordination number, that plays a key role in determining An-O distances. However, despite differences in absolute distance, the trend in values across the series found in the *ab initio* calculations is very similar to the trend observed in our MD simulations (about 0.2 Å from U^{3+} to Lr^{3+}).

C. Hydration enthalpies

Before concluding we investigate the ability of our polarization potential to calculate hydration enthalpies that are reported in the literature.[29,53]

Hydration enthalpies, ΔH_{hydr}, can be estimated from our simulations from the difference between the total energy of the solution and the pure solvent to which several terms have to be added to compare with experimental hydration enthalpies. A first term is simply – 5/2 RT while the remaining terms depend on the treatment of electrostatic interactions and they can be estimated following the works of Garcia, McCammon, and Hünenberger.[81–84] In particular, in the case of Ewald summation we need to include three main corrections due to: (i) the neutralizing background charge assumed in the Ewald sums, $\Delta H_B = -12.28$ kJ/mol, that depends mainly on the charge of the ion and the simulation box length; (ii) an improper summation scheme to evaluate the potential at the ion site, $\Delta H_{C1} = -191$ kJ/mol, that depends on the quadrupole-moment trace of the solvent molecule; (iii) the vacuum to liquid interfacial potential jump, $\Delta H_{C2} = +211$ kJ/mol, that mainly depends on the ion charge.

These corrections were applied and ΔH_{hydr} calculated for all our simulations. Results obtained are reported in Table V where we compare them with literature values. Our CLMD hydration enthalpies show reasonable agreement with the well established old values of Marcus[29] who provided data only for U^{3+} and Pu^{3+}. The resulting hydration enthalpies have differences of about 2% relative to experimental values of Marcus, this difference being similar to what was obtained for other 3+ ions (3%) (Ref. 24) and less than what was obtained in the case of Al^{3+} (10%).[85] If we consider the difference between U^{3+} and Pu^{3+} hydration enthalpies we have a very good agreement with Marcus values (102 vs 90 kJ/mol). Another estimate of hydration enthalpies by David and Vokhmin[53] was obtained by fitting a large set of parameters[86] on various properties (like, e.g., ionic radii and number of water molecules in second hydration shell) using a thermodynamic model for the entire An^{3+} series. They obtained the same decrease as Marcus from U^{3+} to Pu^{3+}, but smaller absolute values. Differences with respect to our results are bigger at the beginning of the series (where we agree with Marcus values) and smaller at the end of the series. Comparing the difference between An^{3+} ions, $\Delta\Delta H_{hydr}$, across the whole series, our CLMD simulations show a smaller decrease than the thermodynamic model for the heaviest An^{3+} ions. Thus the good agreement with our CLMD values for some element (e.g., Cf^{3+} and Lr^{3+}) might be fortuitous. The difference in the trend between our CLMD simulations and the published thermodynamic model is not unexpected, since the thermodynamic model assumes different values for physical parameters employed in the model, especially for effective charges and coordination numbers. For example, by modifying their parameters in a reasonable range, changes of the order of hundreds kJ/mol are obtained. We should note that while David and Vokhmin[53] report a difference in energy between U^{3+} and Lr^{3+} of about 600 kJ/mol, Dolg and coworkers obtained a difference of about 300 kJ/mol from quantum chemical calculations[47] and our simulations provide values between 215 and 399 kJ/mol as a function of the parameter sets employed. Note that changing interaction parameters for a given ion while has a little effect on structure, can result

TABLE V. Hydration enthalpies, ΔH_{hydr} in kJ/mol, obtained from simulations. Results with different parameters sets are shown: r_9, $r_{8.5}$, and r_8. Also literature data are reported.

	r_9	$r_{8.5}$	r_8	Expt.[a]	Therm.[b]
U^{3+}	−3348			−3435	−3177
Np^{3+}	−3447				−3206
Pu^{3+}	−3450			−3525	−3269
Am^{3+}	−3611				−3295
Cm^{3+}	−3447				−3363
Bk^{3+}	−3570	−3284	−3692		−3479
Cf^{3+}	−3606	−3576	−3609		−3585
Es^{3+}	−3455	−3447	−3536		−3641
Fm^{3+}	−3587	−3538	−3581		−3690
Md^{3+}	−3538	−3675	−3535		−3730
No^{3+}	−3565	−3812	−3638		−3769
Lr^{3+}	−3563	−3699	−3747		−3791

[a]Experimental data from Marcus (Ref. 29).
[b]Tabulated values obtained from thermodynamics model from David and Vokhmin (Ref. 53).

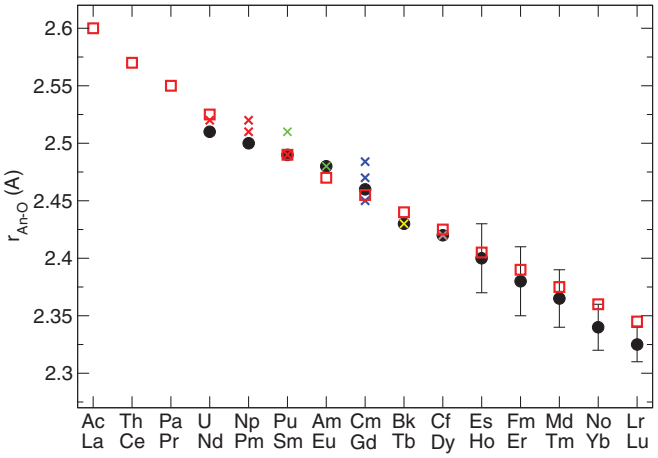

FIG. 5. An-O distances for the whole series (full circles) compared with experimental data (crosses). Experimental Ln-O values obtained by D'Angelo and co-workers (see Ref. 77) are also reported (squares).

in a difference in hydration enthalpy of about 100 kJ/mol (see, e.g., Bk^{3+}, Es^{3+}, Lr^{3+}).

IV. CONCLUSIONS

In this paper we have presented a pair interaction potential including explicit polarization–by means of Thole's induced dipole model–suitable to address key questions about the hydration structure and dynamics of the actinoid(III) series. In particular, the microscopic description obtained from MD simulations seems to be able to clarify some key points that have been debated in the literature regarding the trend of An-O distances and first shell hydration structure across the series.

Our results are able to reproduce correctly An-O distancess obtained by XAS and thus they can be used to better understand these data. Coordination numbers of the actinoids change from 9 to 8 across the series in a similar fashion to what was seen for the lanthanoids(III). A smooth transition between CN = 9 and CN = 8 was obtained between Bk^{3+} and Md^{3+}, that is not so different from the place (Cm^{3+}–Es^{3+}) suggested by some experiments.[53,87,88] Our model, after being compared to and validated by experimental values of the light actinoids, was extended to the last part of the series. In Fig. 5 we summarize our results and compare with the available structural experimental data.

With this model we were able to model the hydration structure of the whole actinoid(III) series. This enables us to compare the water behavior of this series with the lanthanoid(III) series and shed some light on the similarities and differences between hydration structures of the two series (see Fig. 5). This similarity between Ln^{3+} and An^{3+} globally holds, confirming what was suggested by Apostolidis *et al.*[46] and Dupouy *et al.*,[89] for which also the light An^{3+} ions behave similarly to Ln^{3+} reflecting mainly the electrostatic nature of the An-O and Ln-O interaction in liquid water. By inspecting simulation details, we can notice a shift in hydration properties between Ln and corresponding An ions that is not constant across the series from one row position to the other. In fact, while at the beginning we have an almost straight correspondence between each Ln and corresponding An, at the end of the series An-O distances are shorter than corresponding Ln-O ones. This is consistent with the well known stronger An^{3+} contraction compared to Ln^{3+}.[53,66]

Finally, we have checked our force field against hydration energies, that are more "elusive" quantities.[90] Reasonable agreement was obtained between our simulations and literature values.

Concluding, our results can be of help for a deeper understanding of An^{3+} in water in two main ways: (i) using them to better interpret available XAS data of the first half of the actinoid(III) series in water and (ii) allowing the use of the analogy between Ln^{3+} and An^{3+} in a more quantitative way, such that it will be possible to give insights on An^{3+} behavior in water from experiments done on Ln^{3+}, that are often easier to perform.

ACKNOWLEDGMENTS

We thank R. Vuilleumier for useful discussions and J. Beck for careful reading of the manuscript. This work was partially supported by GNR-Paris 2010 (R.S. and P.V.) and ANR JCJC2010 ACLASOLV, Actinoids, and Lanthanoids SOLVation (R.S. and F.M.).

APPENDIX: INTERACTION POTENTIAL DEVELOPMENT

Given two ions of the same series, one for which we have an interaction potential with surrounding molecules (V_{ref}) and the other for which we want to derive a new interaction potential, V_{new}, we can impose that they equalize when

$$V_{ref}(r) = A_{ref} e^{-B_{ref} r} - \frac{C_{ref}}{r^6}, \tag{A1}$$

$$V_{new}(r + \Delta r) = A_{new} e^{-B_{new}(r+\Delta r)} - \frac{C_{new}}{(r + \Delta r)^6}, \tag{A2}$$

where $\Delta r = R_{new} - R_{ref}$. Here R is a not specified parameter length that characterizes the atom. A typical choice (done in our works) is that R is the ionic radius.

Assuming that $A_{ref} = A_{new}$ is a reasonable approximation in the liquid state where A represents the unphysical height of the short range repulsion term that is never reached at liquid conditions, we find

$$e^{-B_{ref} r} = e^{-B_{new}(r+\Delta r)}, \tag{A3}$$

$$\frac{C_{ref}}{r^6} = \frac{C_{new}}{(r + \Delta r)^6}. \tag{A4}$$

The exponential term, can be rewritten as

$$B_{ref} r = B_{new}(r + \Delta r), \tag{A5}$$

$$B_{new} = B_{ref} \left(1 + \frac{\Delta r}{r}\right)^{-1}. \tag{A6}$$

Assuming that $|\frac{\Delta r}{r}| \ll 1$ and expanding in Taylor series, we get

$$B_{new} \simeq B_{ref} - \left(\frac{B_{ref}}{r}\right)\Delta r. \quad \text{(A7)}$$

Proceeding similarly for C_{new}, we find

$$C_{new} \simeq C_{ref}\left(1 + 6\frac{\Delta r}{r}\right), \quad \text{(A8)}$$

where both expansions are truncated at first order.

The two expressions for B and C can be re-written as

$$B_{new} = B_{ref} - k_B(r)\Delta r, \quad \text{(A9)}$$

$$C_{new} = C_{ref} + k_C(r)\Delta r, \quad \text{(A10)}$$

where k_B and k_C are still dependent on r. In our potential, as in standard classical local interaction potentials, B and C are parameters depending only on the nature of the species and thus the r dependence should be removed to have an operative way of using the relationships previously derived. We can remove this r dependence by averaging $k_B(r)$ and $k_C(r)$ over a portion of space of physical relevance. Thus, for $k_B(r)$ we have

$$k'_B = \langle k_B(r)\rangle = \frac{\int_{r_a}^{r_b}\frac{B_{ref}}{r}dr}{(r_b - r_a)} = \frac{B_{ref}\ln(r_b/r_a)}{(r_b - r_a)}, \quad \text{(A11)}$$

for $r_b > r_a$, with $r_b = xr_a$ we can re-write

$$k'_B = B_{ref}\frac{\ln x}{r_a(x-1)}, \quad \text{(A12)}$$

from which we can identify a range of distances where $k'_B = 1$, as found empirically in our previous studies.[7] Solving the equation for two values of r_a (1.0 and 1.5 Å) we have r_b with a value that is in the typical range where non-electrostatic contributions play a role (i.e., about 8.5 and 6.75 Å, respectively).

The same argument holds for C. Note that here and in our previous work,[7] we used a "graphical" method to obtain C values. Inspecting obtained results, we notice that C_{new} varies linearly with Δr,

$$C_{new} = C_{ref} + b\Delta r. \quad \text{(A13)}$$

By linear fitting our values for Ln(III) we found $b = 5.1211 \times 10^4$ kJ mol^{-1} Å^5 and $C_{ref} = 3.7081 \times 10^4$ kJ mol^{-1} Å^6. Thus, we can find as for B, a region where $k'_C = \langle k_C(r)\rangle$ provides the values obtained. In this case, we have r_b of about 11.5 and 9.5 Å for r_a equal to 1.0 and 1.5 Å, respectively.

We have thus shown that there are two approximations behind the choice of deriving new B and C parameters from reference values as a function of a tuning parameter, Δr: (i) Δr must be sufficiently small; (ii) we need to identify a region where the dependence of B_{new} and C_{new} on r can be neglected.

We should point out that this is not a formal derivation but a justification of the approximations used to obtain the new potentials that are mainly based on the fact that this procedure was able to reproduce experimental data, for both lanthanoids(III) (Ref. 7) and actinoids(III).

[1] J. Kemsley, Chem. Eng. News **88**(37), 29 (2010).
[2] N. Kaltsoyannis and P. Scott, *The f Elements, Oxford Chemistry Primers* (Oxford University Press, Oxford, 2007).
[3] D. F. Peppard, P. R. Gray, and M. M. Markus, J. Am. Chem. Soc. **75**, 6063 (1953).
[4] R. Wietzke, M. Mazzanti, J.-M. Latour, J. Pecaut, P.-Y. Cordier, and C. Madic, Inorg. Chem. **37**, 6690 (1998).
[5] V. Philippini, T. Vercouter, and P. Vitorge, J. Solution Chem. **39**, 747 (2010).
[6] B. Allard, H. Kipatsi, and J. O. Liljenzin, J. Inorg. Nucl. Chem. **42**, 1015 (1980).
[7] M. Duvail, P. Vitorge, and R. Spezia, J. Chem. Phys. **130**, 104501 (2009).
[8] L. Helm and A. E. Merbach, Chem. Rev. **105**, 1923 (2005).
[9] I. Persson, P. D'Angelo, S. De Panfilis, M. Sandstrom, and L. Eriksson, Chem. -Eur. J. **14**, 3056 (2008).
[10] M. Duvail, R. Spezia, and P. Vitorge, ChemPhysChem **9**, 693 (2008).
[11] C. Clavaguera, F. Calvo, and J.-P. Dognon, J. Chem. Phys. **124**, 074505 (2006).
[12] Y. Marcus, Chem. Rev. **88**, 1475 (1988).
[13] A. Habenschuss and F. H. Spedding, J. Chem. Phys. **70**, 2797 (1979).
[14] A. Habenschuss and F. H. Spedding, J. Chem. Phys. **70**, 3758 (1979).
[15] T. Yamaguchi, M. Nomura, H. Wakita, and H. Ohtaki, J. Chem. Phys. **89**, 5153 (1988).
[16] W. Meier, P. Bopp, M. M. Probst, E. Spohr, and J. L. Lin, J. Phys. Chem. **94**, 4672 (1990).
[17] L. Helm and A. E. Merbach, Eur. J. Solid State Inorg. Chem. **28**, 245 (1991).
[18] O. V. Yazyev and L. Helm, J. Chem. Phys. **127**, 084506 (2007).
[19] O. V. Yazyev and L. Helm, Theor. Chem. Acc. **115**, 190 (2008).
[20] C. Cossy, L. Helm, and A. E. Merbach, Inorg. Chem. **28**, 2699 (1989).
[21] C. Cossy, L. Helm, and A. E. Merbach, Inorg. Chem. **27**, 1973 (1988).
[22] T. Kowall, F. Foglia, L. Helm, and A. E. Merbach, J. Phys. Chem. **99**, 13078 (1995).
[23] T. Kowall, F. Foglia, L. Helm, and A. E. Merbach, J. Am. Chem. Soc. **117**, 3790 (1995).
[24] A. Villa, B. Hess, and H. Saint-Martin, J. Phys. Chem. B **113**, 7270 (2009).
[25] C. Terrier, P. Vitorge, M.-P. Gaigeot, R. Spezia, and R. Vuilleumier, J. Chem. Phys. **133**, 044509 (2010).
[26] C. Beuchat, D. Hagberg, R. Spezia, and L. Gagliardi, J. Phys. Chem. B **114**, 15590 (2010).
[27] M. Duvail, A. Ruas, L. Venault, P. Moisy, and P. Guilbaud, Inorg. Chem. **49**, 519 (2010).
[28] B. Brendebach, N. L. Banik, C. M. Marquardt, J. Rothe, M. Denecke, and H. Geckeis, Radiochim. Acta **97**, 701 (2009).
[29] Y. Marcus, Biophys. Chem. **51**, 111 (1994).
[30] P. Allen, J. J. Bucher, D. K. Shuh, N. M. Edelstein, and I. Craig, Inorg. Chem. **39**, 595 (2000).
[31] M. Antonio, L. Soderholm, C. W. Williams, J.-P. Blaudeau, and B. Bursten, Radiochim. Acta **89**, 17 (2001).
[32] S. Skanthakumar, M. Antonio, R. Wilson, and L. Soderholm, Inorg. Chem. **46**, 3285 (2007).
[33] R. Revel, C. Den Auwer, C. Madic, F. David, B. Fourest, S. Hubert, J. Du, and L. R. Morss, Inorg. Chem. **38**, 4139 (1999).
[34] P. Lindqvist-Reis, C. Apostolidis, J. Rebizant, A. Morgenstern, R. Klenze, O. Walter, T. Fanghanel, and R. G. Haire, Angew. Chem., Int. Ed. **46**, 919 (2007).
[35] E. Galbis, J. Hernandez-Cobos, C. Den Auwer, C. L. Naour, D. Guillaumont, E. Simoni, R. R. Pappalardo, and E. Sanchez-Marcos, Angew. Chem., Int. Ed. **49**, 3811 (2010).
[36] P. Lindqvist-Reis, R. Klenze, G. Schubert, and T. Fanghänel, J. Phys. Chem. B **109**, 3077 (2005).
[37] P. Lindqvist-Reis, C. Walther, R. Klenze, and N. M. Edelstein, J. Phys. Chem. C **113**, 449 (2009).
[38] B. J. Palmer, D. M. Pfund, and J. L. Fulton, J. Phys. Chem. **100**, 13393 (1996).
[39] P. D'Angelo, V. Barone, G. Chillemi, N. Sanna, W. Mayer-Klauke, and N. Pavel, J. Am. Chem. Soc. **124**, 1958 (2002).
[40] J. L. Fulton, S. M. Kathmann, G. K. Schenter, and M. Balasubramanian, J. Phys. Chem. A **113**, 13976 (2009).

[41]G. Chillemi, P. D'Angelo, N. Pavel, N. Sanna, and V. Barone, J. Am. Chem. Soc. **124**, 1968 (2002).
[42]G. Mancini, N. Sanna, V. Barone, V. Migliorati, P. D'Angelo, and G. Chillemi, J. Phys. Chem. B **112**, 4694 (2008).
[43]P. D'Angelo, V. Migliorati, G. Mancini, V. Barone, and G. Chillemi, J. Chem. Phys. **128**, 84502 (2008).
[44]P. D'Angelo, A. Zitolo, V. Migliorati, G. Mancini, I. Persson, and G. Chillemi, Inorg. Chem. **48**, 10239 (2009).
[45]R. Spezia, M. Duvail, P. Vitorge, and P. D'Angelo, J. Phys. : Conf. Ser. **190**, 012056 (2009).
[46]C. Apostolidis, B. Schimmelpfennig, N. Magnani, P. Lidqvist-Reis, O. Walter, R. Sykora, A. Morgenstern, R. C. E. Colineau, R. Klenze, R. G. Haire, J. Rebizant, F. Bruchertseifer, and T. Fanghanel, Angew. Chem., Int. Ed. **49**, 6343 (2010).
[47]J. Wiebke, A. Moritz, X. Cao, and M. Dolg, Phys. Chem. Chem. Phys. **9**, 459 (2007).
[48]T. Yang and B. E. Bursten, Inorg. Chem. **45**, 5291 (2006).
[49]D. Hagberg, E. Bednarz, N. M. Edelstein, and L. Gagliardi, J. Am. Chem. Soc. **129**, 14136 (2007).
[50]R. Atta-Fynn, E. J. Bylaska, G. K. Schenter, and W. A. de Jong, J. Phys. Chem. A **115**, 4665 (2011).
[51]F. Real, M. Trumm, V. Vallet, B. Schimmelpfennig, M. Masella, and J.-P. Flament, J. Phys. Chem. B **114**, 15913 (2010).
[52]R. Frick, A. B. Pribil, T. S. Hofer, B. R. Randolf, A. Bhattacharjee, and B. M. Rode, Inorg. Chem. **48**, 3993 (2009).
[53]F. H. David and V. Vokhmin, New J. Chem. **27**, 1627 (2003).
[54]B. T. Thole, Chem. Phys. **59**, 341 (1981).
[55]W. L. Jorgensen, J. Chandrasekhar, J. D. Madura, R. W. Impey, and M. L. Klein, J. Chem. Phys. **79**, 926 (1983).
[56]P. van Duijnen and M. Swart, J. Phys. Chem. A **102**, 2399 (1998).
[57]M. Duvail, M. Souaille, R. Spezia, T. Cartailler, and P. Vitorge, J. Chem. Phys. **127**, 034503 (2007).
[58]A. J. Stone, *The Theory of Intermolecular Forces*, International Series of Monographs on Chemistry, 32 (Clarendon, Oxford, 1997).
[59]H. L. Williams, K. Szalewicz, B. Jeziorski, R. Moszynski, and S. Rybak, J. Chem. Phys. **98**, 1279 (1993).
[60]O. Engkvist, P.-O. Astrand, and G. Karlstrom, Chem. Rev. **100**, 4087 (2000).
[61]S. Brdarski and G. Karlstrom, J. Phys. Chem. A **102**, 8182 (1998).
[62]F. Hutchinson, M. Wilson, and P. A. Madden, Mol. Phys. **99**, 811 (2001).
[63]M. Wilson, P. A. Madden, and P. Costa-Cabral, J. Phys. Chem. **100**, 1227 (1996).
[64]M. Salanne, C. Simon, P. Turq, and P. A. Madden, J. Phys. Chem. B **112**, 1177 (2008).
[65]Y. Okamoto, S. Suzuki, H. Shiwaku, A. Ikeda-Ohno, T. Yaita, and P. A. Madden, J. Phys. Chem. A **114**, 4664 (2010).
[66]R. D. Shannon, Acta Crystallogr. Sect. A **32**, 751 (1976).
[67]M. Souaille, H. Loirat, D. Borgis, and M.-P. Gaigeot, Comput. Phys. Commun. **180**, 276 (2009).
[68]M. Sprik, J. Chem. Phys. **95**, 2283 (1991).
[69]U. Essmann, L. Perera, M. L. Berkowitz, T. Darden, H. Lee, and L. G. Pedersen, J. Chem. Phys. **103**, 8577 (1995).
[70]M. Duvail, R. Spezia, T. Cartailler, and P. Vitorge, Chem. Phys. Lett. **448**, 41 (2007).
[71]M. Duvail, P. Vitorge, and R. Spezia, Chem. Phys. Lett. **498**, 90 (2010).
[72]M. J. Frisch, G. W. Trucks, H. B. Schlegel *et al.*, GAUSSIAN 98, Revision A.9, Gaussian, Inc., Pittsburgh, PA, 1998.
[73]X. Cao, M. Dolg, and H. Stoll, J. Chem. Phys. **118**, 487 (2003).
[74]X. Cao and M. Dolg, J. Mol. Struct.: THEOCHEM **673**, 203 (2004).
[75]F. Real, V. Vallet, C. Clavaguera, and J.-P. Dognon, Phys. Rev. A **78**, 052502 (2008).
[76]R. Heyrovska, Chem. Phys. Lett. **429**, 600 (2006).
[77]P. D'Angelo, A. Zitolo, V. Migliorati, G. Chillemi, M. Duvail, P. Vitorge, S. Abadie, and R. Spezia, Inorg. Chem. **50**, 4572 (2011).
[78]D. R. Lide, *Handbook of Physics and Chemistry* (CRC, Boca Raton, FL, 1996).
[79]C. Clavaguera and J. P. Dognon, Chem. Phys. **311**, 169 (2005).
[80]T. Yang, S. Tsushima, and A. Susuki, J. Phys. Chem. A **105**, 10439 (2001).
[81]G. Hummer, L. R. Pratt, and A. E. Garcia, J. Phys. Chem. **100**, 1206 (1996).
[82]P. H. Hünenberger and J. A. McCammon, J. Chem. Phys. **110**, 1856 (1999).
[83]M. A. Kastenholz and P. H. Hünenberger, J. Chem. Phys. **124**, 124106 (2006).
[84]M. A. Kastenholz and P. H. Hünenberger, J. Chem. Phys. **124**, 224501 (2006).
[85]T. M. C. Faro, G. P. Thim, and M. S. Skaf, J. Chem. Phys. **132**, 114509 (2010).
[86]F. H. David and V. Vokhmin, J. Phys. Chem. A **105**, 9704 (2001).
[87]F. H. David and B. Fourest, New J. Chem. **21**, 167 (1997).
[88]B. Fourest, J. Duplessis, and F. David, Radiochim. Acta **36**, 191 (1984).
[89]G. Dupouy, I. Bonhoure, S. D. Conradson, T. Dumas, C. Hennig, C. Le Naour, P. Moisy, S. Petit, A. Scheinost, E. Simoni, and C. Den Auwer, Eur. J. Inorg. Chem. **10**, 1560 (2011).
[90]P. H. Hünenberger and M. M. Reif, *Experimental and Theoretical Approaches to Elusive Thermodynamic Quantities* (Royal Society of Chemistry, Cambridge, 2011).